



# CircPICALM promotes neonatal acute kidney injury triggered by hypoxia/reoxygenation via sponging microRNA-204-5p

Yang Yang<sup>a,1</sup>, Jing-jing Pan<sup>b,\*</sup>, Xiao-qing Chen<sup>b</sup>, Jia Shi<sup>a</sup>, Mu-zi Wang<sup>a</sup>, Tian-yu Liu<sup>a</sup>, Xiao-guang Zhou<sup>a</sup>

<sup>a</sup> Department of Neonatology, Children's Hospital of Nanjing Medical University, Nanjing, Jiangsu 210008, PR China

<sup>b</sup> Department of Neonatology, The First Affiliated Hospital, Nanjing Medical University, Nanjing, Jiangsu 210000, PR China

## ARTICLE INFO

### Keywords:

circRNA  
miR-204-5p  
Acute kidney injury  
Hypoxia/reoxygenation  
Oxidative stress

## ABSTRACT

**Background:** Circular RNAs (circRNAs) have been documented to regulate neonatal acute kidney injury (AKI). Based on previous RNA-sequence findings, circPICALM exhibited significantly disparate expression between AKI newborns and Controls. This study aimed to provide further insights into the regulatory mechanism of circPICALM in neonatal AKI.

**Methods:** C57BL/6 mice born 7 days were divided into Control group and hypoxia groups (11%O<sub>2</sub> and 8%O<sub>2</sub> groups). Human tubule epithelial cells (HK-2) were stimulated with hypoxia/reoxygenation (H/R) to establish an AKI cell model. Through overexpression and knockdown techniques, the regulatory role of circPICALM in H/R-induced kidney injury was explored. Inflammatory cytokines, cell apoptosis, and oxidative stress were also detected to confirm the regulatory function of circPICALM in neonatal AKI.

**Results:** RT-qPCR confirmed that circPICALM was highly expressed in the serum of AKI newborns, neonatal I/R mice and H/R-treated HK-2 cells. Functionally, circPICALM exacerbated H/R-induced HK-2 cell injury by aggravating apoptosis and mitochondrial oxidative stress, increasing the expression of inflammatory factors, including IL-6, IL-1 $\beta$ , and TNF- $\alpha$ . Conversely, inhibition of circPICALM alleviated H/R injury in the HK-2 cell line. The interaction between circPICALM and miR-204-5p was validated through RNA immunoprecipitation and luciferase assay. Finally, circPICALM functioned as a molecular sponge of miR-204-5p and promoted the upregulation of downstream IL-1 $\beta$  expression.

**Conclusion:** CircPICALM plays a critical role in H/R-induced neonatal AKI by sponging miR-204-5p and then activating the downstream IL-1 $\beta$  signaling axis. The inhibition of circPICALM and subsequent suppression of pro-inflammatory factors could serve as a promising biomarker and therapeutic target for early intervention in neonatal AKI.

## 1. Introduction

Acute kidney injury (AKI) in newborns is a severe disease, that affects an estimated 18–70 % of infants in the neonatal intensive care unit (NICU). This ailment is associated with prolonged hospital stay, increased mortality rate, and worse prognosis [1–7]. Neonatal AKI is

generally caused by various risk factors, such as sepsis, nephrotoxic drugs, cardiopulmonary bypass surgery, and perinatal asphyxia (PA). Among them, the occurrence of AKI in neonates induced by PA fluctuates from 11.7 % to 60.0 %, contingent upon the specific diagnostic criteria employed [3,8]. Since 2013, the criteria of neonatal modified Kidney Disease: Improving Global Outcomes (KDIGO) have been

**Abbreviations:** AKI, Acute kidney injury; ANOVA, one-way analysis of variance; CircRNA, Circular RNA; ELISA, Enzyme-linked immunosorbent assay; gDNA, Genomic DNA; H/R, Hypoxia/reoxygenation; I/R, Ischemia-reperfusion; KDIGO, Kidney Disease: Improving Global Outcomes; MDA, Malondialdehyde; MiRNA, MicroRNA; MUT, Mutant; ncRNAs, non-coding RNAs; NC, Negative control; NICU, Neonatal intensive care units; PA, Perinatal asphyxia; PBS, Phosphate-buffered saline; RIP, RNA immunoprecipitation; ROS, Reactive oxygen species; RT-PCR, Real-time polymerase chain reaction; SCr, Serum creatinine; SOD, Superoxide dismutase; UTR, Untranslated region; WT, Wild-type.

\* Corresponding author at: Department of Neonatology, The First Affiliated Hospital, Nanjing Medical University, 368, Jiangdong North Road, Nanjing, Jiangsu, PR China.

E-mail address: [pjj86961@163.com](mailto:pjj86961@163.com) (J.-j. Pan).

<sup>1</sup> Means co-first authors.

<https://doi.org/10.1016/j.bbadis.2025.167795>

Received 18 October 2024; Received in revised form 1 February 2025; Accepted 6 March 2025

Available online 12 March 2025

0925-4439/© 2025 Elsevier B.V. All rights are reserved, including those for text and data mining, AI training, and similar technologies.

utilized to delineate AKI, relying on either the absolute elevation of serum creatinine (SCr) levels or the reduction in urine output [9,10]. However, different from adult or pediatric AKI, the accurate and early diagnosis of neonatal AKI is relatively difficult. Additionally, PA-induced AKI is driven by complex pathophysiological mechanism. Thus, carefully investigating the molecular mechanism underlying neonatal AKI is crucial for identifying innovative approaches to prevent and mitigate neonatal kidney injury.

Circular RNA (circRNA) is one kind of non-coding RNAs with a covalent bond structure, characterized by the absence of a 5' terminal cap and 3' terminal poly (A) tail [11]. Because of the specific circular structure, circRNAs are resistant to nucleases. This kind of small RNA exhibits stability in peripheral blood and exosomes, which is also abundant in the kidney tissue [12]. A key function of circRNAs is to act as microRNA (miRNA) sponges, regulating downstream signaling pathways. A recent report has revealed the involvement of circRNAs in a spectrum of renal diseases, including AKI [13]. For instance, ciRs-126 is a significant indicator of survival in severe AKI patients [14]. In addition, circ\_0023404 exhibits higher expression level in AKI patients as well as in hypoxia/reoxygenation (H/R) cell models. Circ\_0023404 plays a role as a sponge of miR-136 which contributes to the H/R-induced kidney injury [15]. Regarding circPICALM (hsa\_circ\_0023919), in our previous study it showed differential expression in the peripheral blood between hypoxia-induced AKI neonates and controls [16] (Supplementary). So, it was selected for further functional experiments. In other studies, circPICALM is notably downregulated in bladder cancer. It could act as a sponge for miR-1265, then modulating the expression of STEAP4 and influencing FAK phosphorylation, consequently contributing to metastatic processes [17]. Nonetheless, the specific mechanism of circPICALM in neonatal AKI has been unclear.

Given the above, in this study, the expression of circPICALM in PA-induced AKI newborns, animal model, and cell model was detected respectively. Furthermore, an AKI cell model (HK-2 cell line) stimulated by H/R was established to simulate kidney injury after neonatal asphyxia. Then, miR-204-5p was confirmed as a downstream target of circPICALM. And, IL-1 $\beta$  could act as a target of miR-204-5p. In addition, the potential regulatory role of circPICALM/miR-204-5p/IL-1 $\beta$  axis in the progression of PA-induced AKI was explored in vitro.

## 2. Material and methods

### 2.1. Patient samples

From October 2020 to November 2021, AKI blood samples were taken from newborns in the NICU of the First Affiliated Hospital of Nanjing Medical University. For the AKI group, peripheral blood was drawn when AKI was diagnosed. For the control group, blood samples were taken from newborns with physiological jaundice (mild to moderate indirect hyperbilirubinemia) on the third day after birth. Firstly, five samples from the AKI group ( $n = 5$ ) and five samples from the control group ( $n = 5$ ) were pooled into two independent tubes for high-throughput sequencing. Secondly, peripheral blood samples were collected for q-PCR validation from another 20 asphyxial AKI newborns and another 16 controls (neonates with physiological jaundice) (Supplementary) [16].

### 2.2. Estimation of sample size

As shown in the previous high-throughput sequencing results (Supplementary), the  $|\text{Log}_2 \text{ Fold Change}|$  of circPICALM in the AKI group was about 4.26 times higher than in the control group. The standard deviation ( $\sigma$ ) of the circPICALM expression level was 1.283. Considering  $\alpha = 0.05$  and  $\beta = 0.20$ , if a 1:1 design was adopted between the AKI group and the control group, it is calculated that at least 4 infants (AKI group  $n = 2$ , Control group  $n = 2$ ) are needed for further q-PCR validation after calculating by R statistical software (version 4.3.1). In fact,

in this study 20 asphyxial AKI newborns and 16 controls were subsequently enrolled in this study (Supplementary).

### 2.3. Diagnostic criteria

The criteria for acute perinatal asphyxia included: (a) signs of fetal distress such as late decelerations, bradycardia, and loss of heart rate variability; (b) the onset of a significant hypoxic event before or during delivery; (c) clinical presentation of hypoxic-ischemic encephalopathy and involvement of multiple secondary organs; and (d) detection of severe acidosis in umbilical artery blood, characterized by  $\text{pH} \leq 7.0$  with base deficit  $\geq -16$  mmol/l [18]. The definition of AKI followed the neonatal modified KDIGO criteria [9], which involved either a sustained elevation of SCr levels exceeding 1.5 mg/dl for a minimum of 24 h, or a reduced urine output of  $<1.0$  ml/kg\*h.

### 2.4. Animal experiments

C57BL/6 mice born 7 days were randomly divided into three groups: Control group, hypoxia groups (11%O<sub>2</sub> group and 8%O<sub>2</sub> group), the number of each group was 6. In the hypoxia groups were subjected for 2 h of systemic hypoxia in anoxic incubator in an atmosphere containing 8 % oxygen and 92 % nitrogen or 11 % oxygen and 89 % nitrogen at a temperature of 37 °C. After exposure, the animals were returned to their mothers and after 2 h reoxygenation, kidneys were taken for further examination.

### 2.5. Cell culture and hypoxia/reoxygenation (H/R) treatment

The human renal proximal tubular cell line (HK-2 cell line, Cat. FH0228) (Fuheng Institutes for Biological Sciences, Shanghai, China) was cultured in Dulbecco's Modified Eagle Medium/Nutrient Mixture F12 (DMEM/F12, Gibco) containing 10 % fetal bovine serum (Gibco, China) and penicillin/streptomycin (100 U/ml) at 37 °C with 5 % CO<sub>2</sub>. HK-2 cell line stimulated by H/R was established to simulate the environment of kidney injury after neonatal asphyxia. For detailed H/R treatment, cells were cultured in a serum-free medium and transferred to hypoxic conditions (5 % CO<sub>2</sub>, 1 % O<sub>2</sub>, and 94 % N<sub>2</sub>) for four time intervals (0, 12, 18, and 24 h), after which they were reoxygenated for 2 h in fresh normal medium, constituting the H/R group. For further study, HK-2 cells were cultured in hypoxia conditions for 18 h and reoxygenated for 2 h to establish H/R model.

### 2.6. Cell transfection

Lentivirus packaging cells (GeneChem, China) were transfected with lentivirus silencing hsa\_circ\_0023919 (sh-anti-hsa\_circ\_0023919), lentivirus overexpressing hsa\_circ\_0023919 (LV-hsa\_circ\_0023919), or the negative control (sh-anti-NC or LV-NC) for 72 h. H/R treatment was conducted after 72 h post-infection. In addition, HK-2 cells cultured in a six-well plate were transfected with 5  $\mu$ l of inhibitor or 3  $\mu$ l of mimic (RiboBio, China) with miR-204-5p using Lipofectamine 2000 (Invitrogen, Thermo Fisher Scientific, China). At 24 h post-transfection, the medium was refreshed.

### 2.7. Quantitative real-time polymerase chain reaction (RT-qPCR)

Total RNA samples were collected from the peripheral blood of included infants, and HK-2 cells were extracted by TRIzol reagent (TaKaRa, Japan) following the manufacturer's instructions. RNA was quantified and reversely transcribed into cDNA (Vazyme, China). For miRNAs, cDNA was synthesized using the PrimeScript™ RT reagent kit (RiboBio, China). RT-qPCR was conducted on a LightCycler480II (Roche, China) using SYBR Green PCR Master Mix (Vazyme, China). The expression level of the target gene was normalized to that of GAPDH and calculated through the  $2^{-\Delta\Delta C_t}$  method. Primers for miR-204-5p, U6, and

circPICALM were procured from RiboBio (China). The specific primer sequences for qPCR are listed in Table 1.

## 2.8. Nuclear-cytoplasmic fractionation and RNase R digestion

Based on the manufacturer's instructions, nuclear and cytoplasmic RNA was isolated using the PARIS kit (Invitrogen, USA). In terms of RNase R treatment, 5 µg of total RNA was digested with 10 U RNase R (Genesee, China) at 37 °C for 30 min. Subsequently, the separated RNA was used for RT-qPCR analysis to detect the circPICALM expression, with GAPDH and U6 as the internal references in the nucleus and cytoplasm, respectively.

## 2.9. RNA immunoprecipitation (RIP) assay

The RIP assay was performed by the Magna RIP™ RNA Binding Protein Immunoprecipitation Kit from Millipore (USA). HK-2 cell lysates were incubated overnight with RIP buffer which contained magnetic beads conjugated with either human anti-AGO2 antibody or negative control rabbit IgG. On the next day, the reaction mixture was treated with Proteinase K for 30 min, and the immunoprecipitated RNA was isolated. RT-qPCR was then conducted to assess the expression levels of circPICALM and miR-204-5p.

## 2.10. Luciferase reporter assay

In terms of luciferase reporter assays, the mutant (MUT) or wild-type (WT) sequence of circPICALM or IL-1β containing the binding sites for miR-204-5p were subcloned into pGL3 basic reporter vectors (Promega, USA). In brief, HK-2 cells were transfected with pGL3-circPICALM WT/MUT or pGL3-IL-1β WT/MUT 3'-untranslated region (UTR) constructs along with miR-204-5p mimics or negative control (NC) mimics. Subsequently, the Dual-Luciferase Assay System (Promega, USA) was utilized to measure luciferase activity.

## 2.11. Flow cytometry assay

Apoptosis was measured using the Annexin V-FITC/PI apoptosis kit (BD Pharmingen™, USA) according to the manufacturer's protocol. The cells were collected after H/R treatment, washed twice with cold phosphate-buffered saline (PBS), and resuspended in binding buffer at a concentration of  $1 \times 10^6$  cells/ml. Subsequently, the cells were stained with 5 µl Annexin V-FITC and 10 µl PI in the dark for 15 min before analysis using flow cytometry (BD, USA). Briefly, forward scattering (FSC) and lateral scattering (SSC) gates were set to preliminary differentiate cell populations. In the FSC vs. SSC scatter plot, circle the target cell population. Distinguish cells in Annexin V vs. PI diagram: Annexin V−/PI−: living cells; Annexin V+/PI−: early apoptotic cells; Annexin V+/PI+: late apoptotic or necrotic cells. Apoptosis rate was the

percentage of late apoptotic (Annexin V+/PI+) and early apoptotic (Annexin V+/PI−) cells to cells.

## 2.12. Enzyme-linked immunosorbent assay (ELISA)

Inflammatory factors, such as IL-6, IL-1β, and TNF-α in supernatants of HK-2 cells were detected using the IL-6 (Item number: E-EL-H6156), IL-1β (Item number: E-EL-H0149), and TNF-α (Item number: E-EL-H0109) ELISA kits (Elabscience, China), respectively. The absorbance at 450 nm was measured on a Microplate Luminescence Detector (Promega GloMax, USA).

## 2.13. Oxidative stress assay

The oxidative stress assay was conducted by assessing the activities of various oxidative indicators. Levels of malondialdehyde (MDA) and reactive oxygen species (ROS) were measured using the ROS or MDA assay kit from Beyotime (China). Activities of superoxide dismutase (SOD) and L-glutathione (GSH) were determined using the SOD assay kit (Beyotime, China) and the GSH assay kit (Jiancheng, China), respectively, following the manufacturer's protocols.

## 2.14. Bioinformatics

The information of circPICALM was searched on circBase (<http://www.circbase.org>). The potential miRNAs targeted by circPICALM were predicted using the bioinformatics resources starBase (<http://starbase.sysu.edu.cn/>) and circBank (<http://www.circbank.cn/>). The potential miRNAs bound to IL-1β were also predicted using starBase (<http://starbase.sysu.edu.cn/>).

## 2.15. Statistical analysis

1) In terms of the comparison of clinical characteristics between AKI patients and controls, quantitative data were manifested as mean and standard deviation (SD). Comparisons between the two groups were performed using the *t*-test. For qualitative data, the Pearson Chi-square test or Fisher's exact test was conducted. 2) As far as the cell and animal experiments in this study as concerned, the quantitative variables were shown as mean ± standard error (SE), and were conducted at least three times. Differences between the two groups were evaluated for significance through a Student's *t*-test (two-tailed), while comparisons among multiple groups were analyzed by one-way analysis of variance (ANOVA). Statistical analysis was implemented using GraphPad Prism version 8.0 software. A *P* < 0.05 was considered statistically significant in this study.

## 3. Results

### 3.1. Expression of circPICALM in the peripheral blood of AKI patients, neonatal I/R mice and H/R-treated cells

Firstly, RNA high-throughput sequencing data of peripheral blood were analyzed between PA-induced AKI neonates and controls [16]. Compared to the non-AKI group, the results showed a total of 186 upregulated circRNAs (Fold change > 2 and *P* < 0.05) in the AKI group (Supplementary) [16]. Among them, circPICALM (has\_circ\_0023919) exhibited higher expression in the peripheral blood of PA-AKI neonates (Fig. 1A–B). In neonatal I/R mice, histological study revealed slight changes in kidney morphology induced by hypoxia (Fig. 1C), but RT-qPCR showed kidney injury biomarkers: NGAL and KIM-1 increased significant in 8%O<sub>2</sub> group (Fig. 1D). Results showed circPICALM were upregulated in 8%O<sub>2</sub> group (Fig. 1E). To further verify whether the expression of circPICALM was induced by hypoxia injury, an in vitro cell model of H/R-triggered AKI was established (Fig. 1F–G), and the results validated that the circPICALM level was also significantly elevated in the

**Table 1**  
Primer sequences.

Gene	Primer sequences(5' → 3')
hsa_circ_0023919	F:TAGCAAGTACATGGGAGGCC R:CATTGGAAGTGTAGTTGCCCT
GAPDH	F:GAACGGGAAGCTCACTGG R:GCCTGCTTCAACACCTTCT
IL-1β	F:TTGAGTCTGCCAGTTCC R:TTTCTGCTTGAGAGGTGCT
IL-6	F:CAATAACCAACCCCTGACC R:GCGCAGAATGAGATGAGTT
TNFα	F:GGAAAGGACACCATGAGC R:CCACGATCAGGAAGGAGA
BAX	F:GCGACTGATGTCCCTGTCT R:TGAGTGAGGCGGTGAGC
BCL-2	F:GCGGATTGACATTCTGTG R:CATAAGGCAACGATCCCA

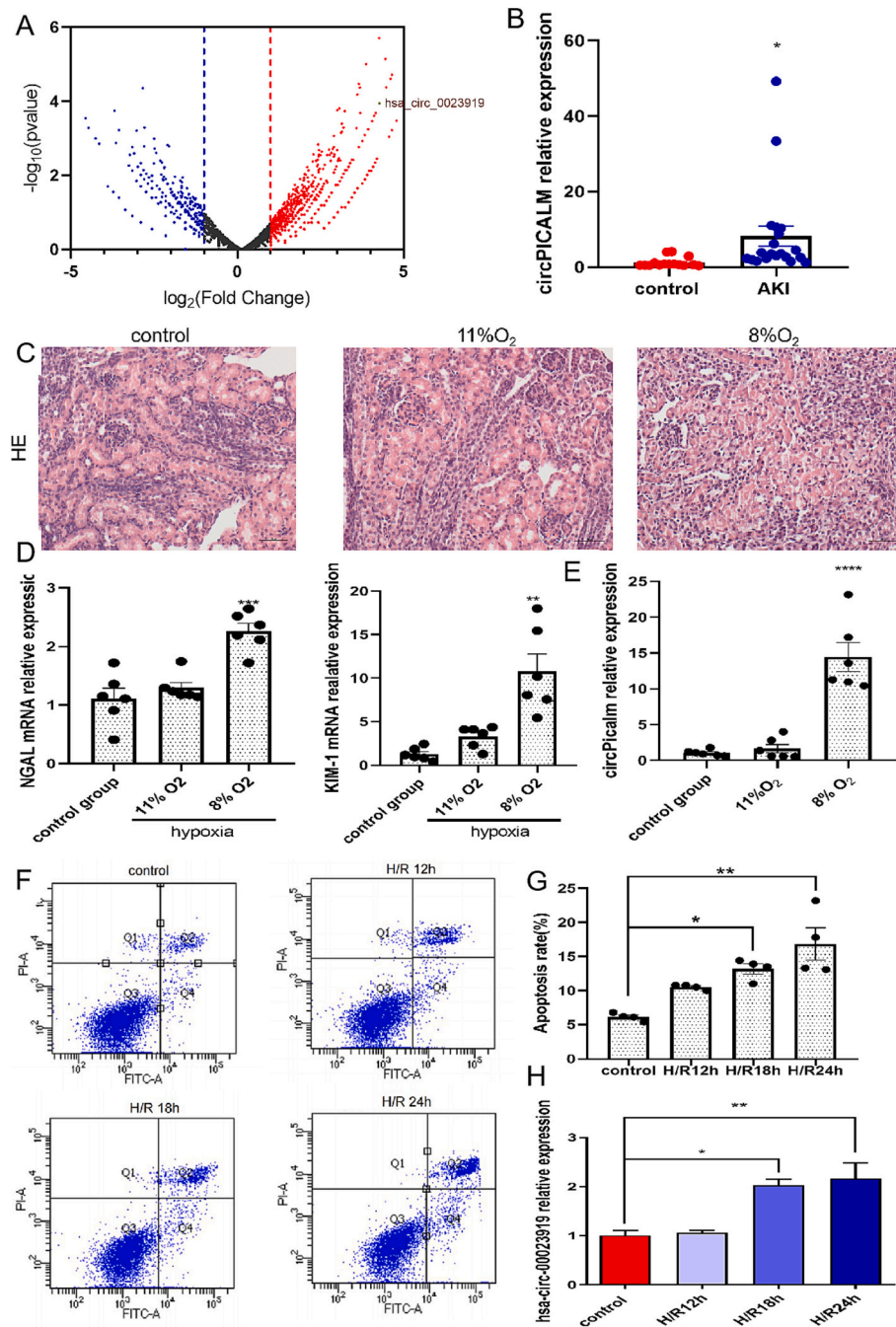


**Fig. 1.** Expression of circPICALM in the peripheral blood of AKI patients, neonatal I/R mice and H/R-treated cells. **A.** RNA high-throughput sequencing exhibited differential circRNA expression between AKI and control groups. Red dot: upregulated expression; blue dot: downregulated expression. **B.** RT-qPCR exhibited circPICALM expression in PA-AKI and healthy control neonates. **C.** Histological examination of kidney morphology in different groups. **D.** NGAL and KIM-1 mRNA expression in hypoxia mice; **E.** circPICALM expression in hypoxia mice; **F–G.** Flow cytometry evaluated cell apoptosis in HK-2 cells under H/R treatment at different time points. **H.** RT-qPCR exhibited circPICALM expression in H/R-triggered HK-2 cells. \* $P < 0.05$ ; \*\* $P < 0.01$ . (For interpretation of the references to colour in this figure legend, the reader is referred to the web version of this article.)

H/R group in a time-dependent manner (Fig. 1H). The above results indicated that the expression of circPICALM was increased not only in the peripheral blood of AKI neonates but also in vivo and in vitro AKI models. According to circbase2.0, circPICALM has a genomic length of 6626 nt and a spliced length of 451 nt; and the genomic location is chr11:85707868-85714494 ([http://www.circbase.org/cgi-bin/singlerecord.cgi?id=hsa\\_circ\\_0023919](http://www.circbase.org/cgi-bin/singlerecord.cgi?id=hsa_circ_0023919)).

### 3.2. The looping and localization characteristics of circPICALM in HK-2 cells

The RNase R assay in HK-2 cells exhibited a decreased expression of linear PICALM mRNA due to RNase R digestion, while the circPICALM expression was not affected (Fig. 2A). The stability of circPICALM was detected by PCR through cDNA and genomic DNA (gDNA) untreated or pretreated with RNase R (Fig. 2B). CircPICALM was resistant to digestion under RNase R treatment, while the linear form of PICALM was digested. gDNA did not present a circRNA amplification product

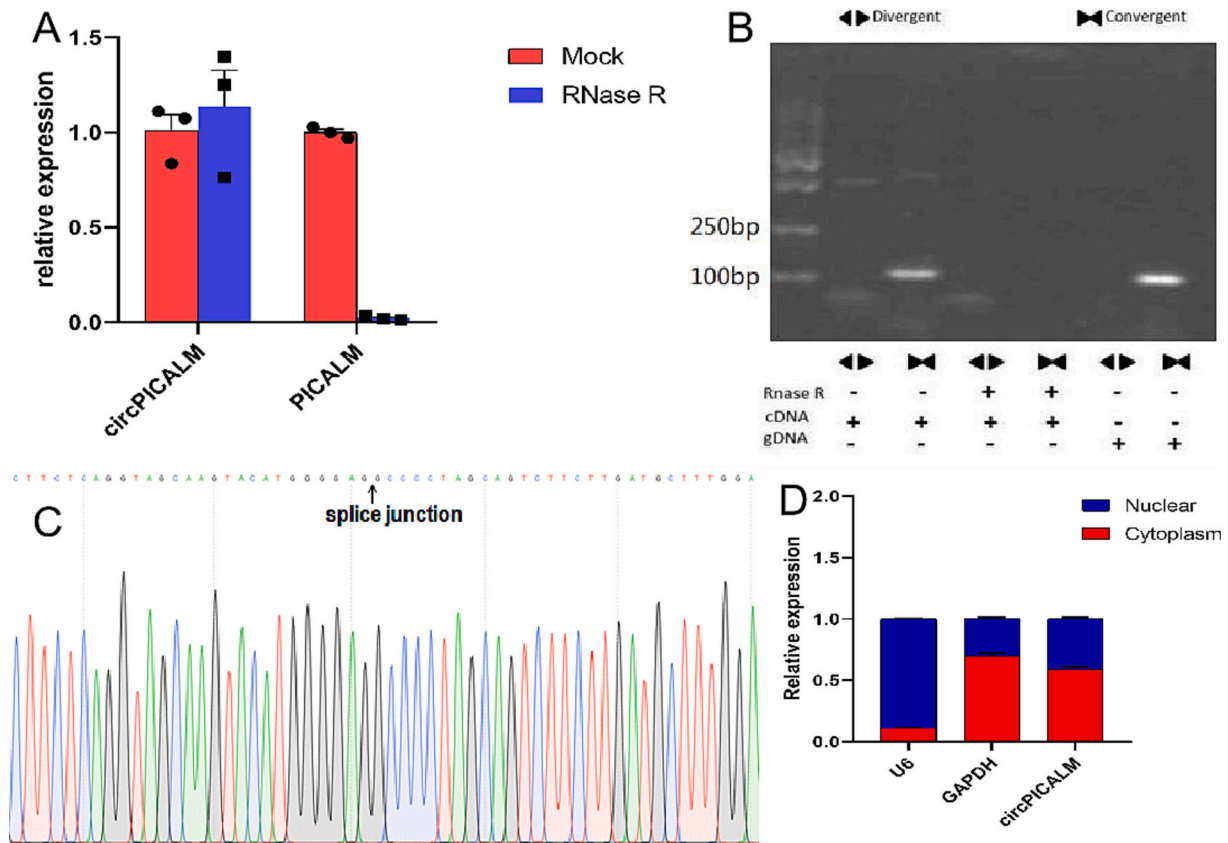


**Fig. 2.** The looping and localization characteristics of circPICALM in HK-2 cells. **A.** RT-qPCR exhibited circPICALM and linear PICALM levels in HK-2 cells after RNase R treatment. **B.** Linear and anti-splice products were amplified by polymerase chain reaction primers regardless of treatment with RNase R. **C.** Identification of circPICALM splice junction. **D.** RT-qPCR confirmed that circPICALM and PICALM are located in the cytoplasm of HK-2 cells.

compared to cDNA. Detection of the splice junction sequence also confirmed the circular structure of circRNA (Fig. 2C). Such results demonstrated that circPICALM was a stable circular RNA. After the physical separation of nucleoli and cytoplasmic RNA, RT-qPCR showed that circPICALM was mainly localized in the cytoplasm (Fig. 2D).

### 3.3. Interference of circPICALM alleviated H/R-induced HK-2 cell apoptosis

To investigate the function of circPICALM in AKI, circPICALM was overexpressed or knocked down in HK-2 cells (Fig. 3A). The RT-qPCR demonstrated that the expression of circPICALM was downregulated by sh-circPICALM-03 (Fig. 3B). After transfection, cells were treated under an H/R environment. Flow cytometry results indicated that HK-2 cell apoptosis was aggravated in HK-2 cells with the enforced expression of circPICALM (Fig. 3C–D). RT-qPCR results also confirmed that circPICALM overexpression upregulated the levels of pro-apoptotic BAX but suppressed the expression of BCL-2 under H/R treatment. Nonetheless, the phenomena were reversed following the knockdown of circPICALM (Fig. 3E).

### 3.4. The knockdown of circPICALM reduced H/R-induced inflammation and oxidative stress

Further investigation was conducted to determine whether circPICALM was involved in inflammation and oxidative stress under the H/R condition. ELISA and RT-qPCR results revealed that IL-6, IL-1 $\beta$ , and TNF- $\alpha$  were elevated following circPICALM overexpression, which was rescued by circPICALM knockdown (Fig. 4A–B). Then, the oxidative stress indicators in HK-2 cells were determined. Findings were made that overexpression of circPICALM strongly increased the ROS generation

and MDA content but decreased the activity of the antioxidant enzymes SOD and GSH. In addition, the inhibition of circPICALM suppressed the oxidative stress progression (Fig. 4C–D). The described findings suggest that the downregulation of circPICALM relieved H/R-induced HK-2 cell injury by reducing inflammation and oxidative stress levels.

### 3.5. CircPICALM could act as a sponge of miR-204-5p

Previous studies have manifested that circPICALM is mainly localized in the cytoplasm. In the present study, it was hypothesized that circPICALM could be a miRNA sponge to promote the expression of target genes. To predict the target miRNA of circPICALM, starBase (<http://starbase.sysu.edu.cn/>) and circBank (<http://www.circbank.cn/>) were employed together. A total of 13 miRNAs were predicted to interact with circPICALM (Fig. 5A). The top five miRNAs were screened to analyze whether they were associated with kidney injury in H/R-induced HK-2 cell and AKI patients (Fig. 5B–C). Finally, it was predicted that miR-204-5p could be a key molecular player related to circPICALM. Therefore, HK-2 cells were subjected to an anti-AGO2 RIP assay following H/R treatment, wherein an anti-AGO2 antibody (with IgG serving as a negative control) was employed to capture circPICALM and miR-204-5p. The RIP outcomes revealed that both circPICALM and miR-204-5p were enriched by anti-AGO2 antibodies, while no enrichment was observed with non-specific anti-IgG antibodies (Fig. 5D). Additionally, the dual-luciferase reporter assay showed that the intensity of the luciferase reaction was significantly reduced after binding of circPICALM to miR-204-5p (Fig. 5E–F). Meanwhile, circPICALM augmentation decreased the miR-204-5p level in HK-2 cells (Fig. 5G). As such, circPICALM bounded to and negatively regulated miR-204-5p in HK-2 cells.

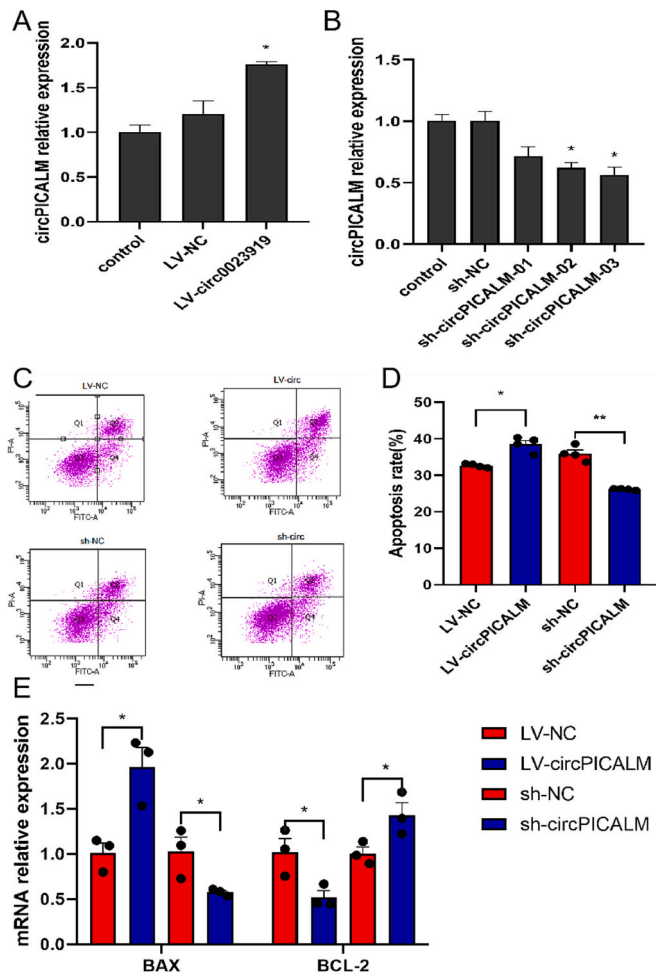


**Fig. 3.** Interference of circPICALM alleviated H/R-induced HK-2 cell apoptosis. A–B. RT-qPCR detected the efficiency after lentivirus transfection. C–D. Flow cytometry evaluated cell apoptosis in HK-2 cells treated with LV-NC, LV-circPICALM, sh-NC, and sh-circPICALM under H/R treatment. E. RT-qPCR analysis of pro-apoptotic BAX and anti-apoptotic BCL-2 expression. \* $P < 0.05$ ; \*\* $P < 0.01$ .

### 3.6. The miR-204-5p mimics attenuated H/R-induced HK-2 cell apoptosis

Further, miR-204-5p mimics and inhibitors were used to enhance or knockdown miR-204-5p expression in HK-2 cells (Fig. 6A). CircPICALM expression was downregulated in miR-204-5p mimic HK-2 cells (Fig. 6B). Flow cytometry and RT-qPCR results revealed that miR-204-5p augmentation significantly alleviated apoptosis (Fig. 6C–D), decreased BAX and BCL-2 expression induced by H/R, while miR-204-5p inhibitors promoted the aggravation of apoptosis (Fig. 6E).

### 3.7. The miR-204-5p mimics attenuated H/R-induced HK-2 cell inflammation and oxidative stress

Similarly, the overexpression of miR-204-5p alleviated oxidative stress and reduced the level of inflammatory cytokines, such as IL-6, IL-1 $\beta$ , and TNF- $\alpha$ , while the downregulation of miR-204-5p exhibited opposite results (Fig. 7A–B). Meanwhile, miR-204-5p mimics also increased the activity of SOD and GSH level, decreased ROS generation and MDA content (Fig. 7C–D).

### 3.8. IL-1 $\beta$ as a target of miR-204-5p

To further explore the potential downstream target of miR-204-5p, a

potential binding site for miR-204-5p in the 3'-UTR of IL-1 $\beta$  was predicted through bioinformatics (Fig. 8A). Luciferase reporter assay showed that miR-204-5p mimic significantly reduced the luciferase activity of WT in HK-2 cells, while the expression level of Mut did not exhibit any changes in luciferase activity (Fig. 8B).

### 3.9. Rescue experiment of circPICALM/miR-204a-5p/IL-1 $\beta$ axis

To further investigate whether circPICALM promotes the biological progress of AKI through the circPICALM/miR-204a-5p/IL-1 $\beta$  axis. HK-2 cells were co-transfected with miR-204-5p mimic and circPICALM overexpression lentivirus. As demonstrated by qPCR analysis, there was a significant reduction in IL-1 $\beta$  mRNA expression upon miR-204-5p overexpression. Upregulating circPICALM rescued the expression of IL-1 $\beta$  (Fig. 9A). In addition, miR-204-5p mimics repressed HK-2 cell apoptosis triggered by H/R, which was reversed by circPICALM overexpression (Fig. 9B–C).

## 4. Discussion

Newborns affected by severe PA commonly experience multi-organ dysfunction. There's a redistribution and adjustment of cardiac output aimed at preserving perfusion to vital organs such as the brain, heart, and adrenal glands, thereby decreasing oxygen perfusion to the kidneys [19]. Previous studies have shown that severe AKI is associated with longer hospital stays and poor clinical outcomes in neonates. Newborns with AKI in the first week of life are related to higher mortality [20–22]. Hence, searching for key mechanisms at the initial stage of AKI is essential for early intervention to prevent the progression of renal tubular cell injury and preserve renal function. Currently, some studies have indicated that oxidative stress and inflammatory response play significant roles in the development of AKI [23].

Furthermore, increasing research has reported that non-coding RNAs (ncRNAs) play a crucial role in regulating kidney diseases. Among the ncRNAs, circRNAs are enriched in the kidney and could function through competitive binding of miRNAs, regulation of various transcriptional processes, or translation of proteins [24]. For example, Shi et al. found that circYAP1 attenuates renal tubular epithelial cells from ischemia-reperfusion (I/R) injury via sponging miR-21-5p and activating the PI3K/AKT/mTOR pathway [25]. Moreover, an in vivo study showed that the expression of circ-AKT3, circ-DNMT3A, circ-plekha7, and circ-ME1 were downregulated in SD rats with I/R AKI, while losartan restored the expression of these circRNAs [26].

In the present study, high-throughput circRNA sequencing was employed to identify differentially expressed circRNAs in AKI newborns (Supplementary). The analysis results revealed that circPICALM was not only upregulated in the serum of newborns with PA-induced AKI but also in H/R-treated HK-2 cell model. Furthermore, the overexpression of circPICALM promoted cell apoptosis and heightened oxidative stress and inflammatory response, whereas the knockdown of circPICALM alleviated H/R-induced injury. CircRNAs can potentially bind miRNAs to regulate downstream signaling mRNA. Consequently, through RIP analysis and luciferase reporter assays, the underlying pathway of circPICALM/miR-204-5p/IL-1 $\beta$  was elucidated. Overall, the current research results indicate that the lack of circPICALM could protect HK-2 cells from H/R-induced injury.

As for miR-204-5p, it was found that it can be secreted by renal tubular epithelial cells [27]. Dong J et al. further found delivering miR-204-5p mimics increased miR-204-5p expression, improved renal function, inhibited renal fibrosis and oxidative stress, and restored autophagy in db/db mice [28]. In contrast, Cheng Y et al. reported that kidneys of patients with hypertension, hypertensive nephrosclerosis, or diabetic nephropathy all exhibited a significant decrease in miR-204-5p. And inhibiting miR-204-5p or deleting the Mir204 gene could lead to the upregulation of the target gene SHP2 [29]. These studies reveal that an appropriate level of miR-204-5p is necessary for maintaining the normal

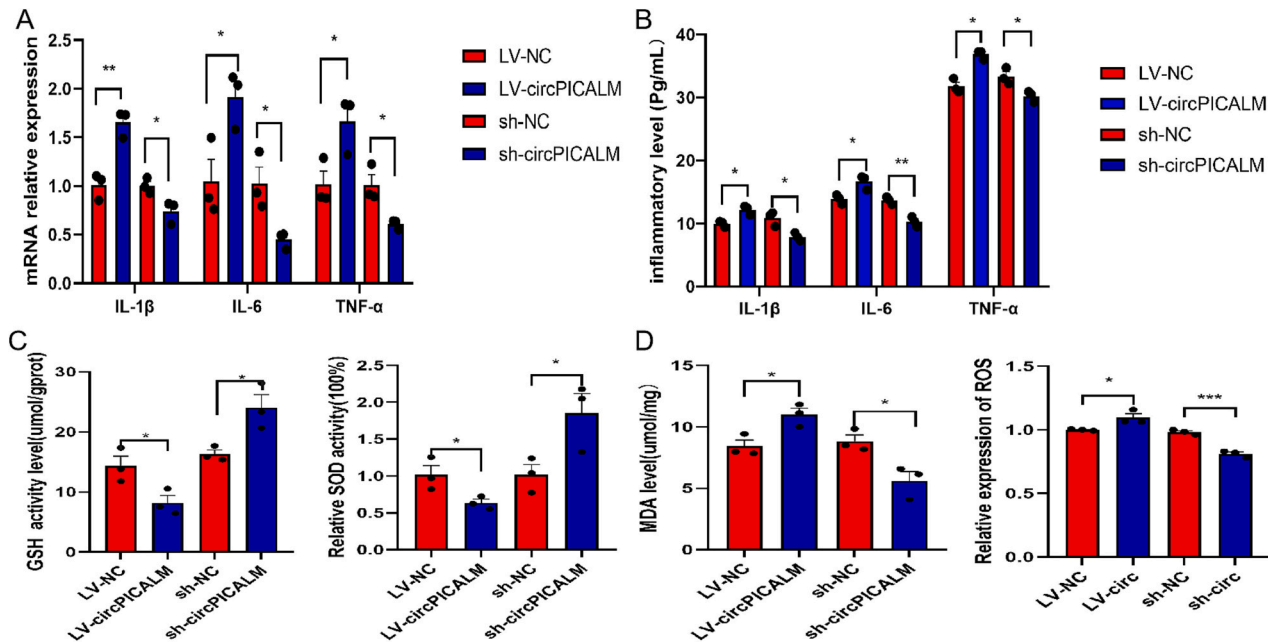


**Fig. 4.** The knockdown of circPICALM reduced H/R-induced inflammation and oxidative stress. A. RT-qPCR exhibited the mRNA levels of IL-1 $\beta$ , IL-6, and TNF- $\alpha$  in HK-2 cells after lentivirus transfection. B. ELISA analysis of the concentration of IL-1 $\beta$ , IL-6, and TNF- $\alpha$  in HK-2 cells after lentivirus transfection. C. Levels of antioxidant enzymes GSH and SOD in HK-2 cells after lentivirus transfection. D. Levels of MDA and ROS in HK2 cells were measured using the corresponding kits. \* $P < 0.05$ ; \*\* $P < 0.01$ ; \*\*\* $P < 0.001$ .

function of renal tubular cells. Furthermore, Li H et al. found the expression of miR-204-5p was downregulated in response to exogenous pro-inflammatory stimulus, TNF- $\alpha$ , or IL-1 $\beta$ , while that of IL-6R was upregulated in HK-2 cells [30]. This study suggests that the expression of inflammatory factors is closely related to miR-204-5p.

In fact, inflammatory factors such as TNF- $\alpha$ , IL-1 $\beta$ , and IL-6 have been implicated in neonatal diseases, with strong evidence suggesting their direct or indirect involvement in renal function impairment in perinatal asphyxia neonates. For instance, previous research has revealed an increased gene expression of renal proinflammatory cytokines (IL-1 $\beta$ , IL-6, TNF- $\alpha$ , and monocyte chemoattractant protein-1) and kidney injury markers promptly after perinatal asphyxia [31]. As a key pro-inflammatory cytokine, IL-1 $\beta$  binds to IL-1 $\alpha$  and activates the same receptor when the kidney undergoes ischemia and hypoxia, subsequently activating the release of other pro-inflammatory cytokines, including IL-6 and TNF- $\alpha$ , which ultimately contributes to final kidney injury. Chen Y further found that following AKI, the canonical pro-inflammatory cytokine IL-1 $\beta$  is released predominantly from activated renal myeloid cells and binds to the IL-1R1 on kidney parenchymal cells. And IL-1R1 could serve as a critical negative feedback regulator of IL-1 signaling in CD11c+ myeloid cells to dampen inflammation to limit AKI [32]. Consequently, early intervention to block the activity and inhibit the release of inflammatory factors plays a crucial role in controlling renal cellular damage [33]. In the present study, IL-1 $\beta$  was significantly upregulated following circPICALM overexpression in HK-2 cells. Compared with that, knockdown of circPICALM could downregulate the expression of IL-1 $\beta$ . These findings highlight the significant roles of circPICALM in the downstream regulation of inflammatory progression in kidney injury.

As far as circRNAs are concerned, Liao Y et al. reported that circRNA\_45478 mediated the progression of ischemic AKI (mouse proximal tubule-derived cell lines) by regulating miR-190a-5p/PHLPP1 axis [34]. A study from Li P et al. revealed that circNRIP1 depletion ameliorated LPS-induced HK-2 cell damage by regulating the miR-339-5p/OXSR1 pathway [35], which suggests the association between circRNAs and oxidative stress. Moreover, Ye W et al. found circ-ITCH could act as a sponge for miR-214-3p, thereby upregulating ABCA1

expression. However, the miR-214-3p inhibitor repressed oxidative stress, inflammation, and mitochondrial dysfunction, which was reversed by circ-ITCH knockdown [36]. This study further proved that the circRNA-miR axis is involved in mitochondrial dysfunction by regulating oxidative stress. In contrast, circPICALM has not been described in kidney diseases yet. Existing evidence only suggests that circPICALM was potentially related to Alzheimer's disease and bladder cancer [37,38]. Our study is the first to report the role of circPICALM in regulating mitochondrial oxidative stress and renal damage. In this study, miR-204-5p was indicated to interact with circPICALM in AKI. Overexpressed miR-204-5p alleviated H/R-induced cell inflammation, apoptosis, and mitochondrial oxidative stress. Further, IL-1 $\beta$  was identified as the downstream target gene of miR-204-5p. The above results collectively demonstrate that circPICALM participates in H/R-induced AKI by targeting the miR-204-5p/IL-1 $\beta$  axis and activating mitochondrial oxidative stress. Therefore, it can be inferred from the results that overexpression of circPICALM could make the signaling axis a potential intervention target for neonatal AKI, thereby reducing the release of inflammatory factors and improving clinical prognosis.

## 5. Limitations

The main limitation is that this study was mainly conducted in vitro, although some in vivo phenotype experiments had been performed. Thus, the mechanism of the circPICALM-miR-204-5p-IL-1 $\beta$  axis could be further elucidated using mammalian in vivo models like neonatal I/R C57BL/6 mice. In I/R mice model, we plan to use lentiviral vector to overexpress or knockdown circPICALM through the tail vein injection. Additionally, circPICALM could be a potential intervention target of PA induced AKI through further experiments like CRISPR-Cas9. It will help us to explore how circPICALM acts on the internal mechanism of mitochondrial oxidative stress. Moreover, Functional validation is also important in different AKI animal models (nephrotoxic drugs, severe infection), which could comprehensively demonstrate that the circPICALM-miR-204-5p-IL-1 $\beta$  signaling axis plays an important role not only in AKI caused by hypoxia. And, inflammatory factors like IL-1 $\beta$ , IL-6, and TNF- $\alpha$  could be detected in these models and informative cells. Last but

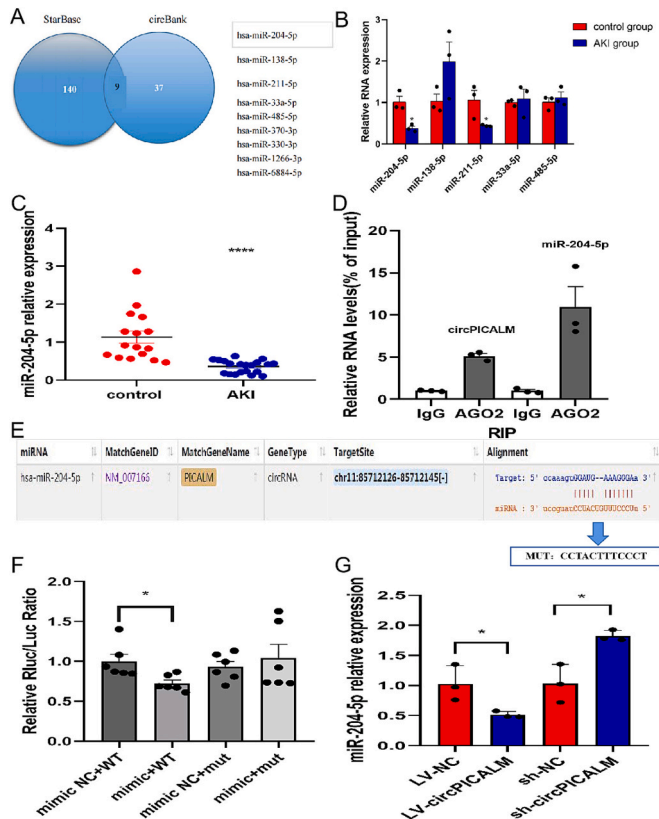


**Fig. 5.** CircPICALM acts as a sponge for miR-204-5p in HK-2 cells. A. Prediction of downstream target miRNA by circBank and starBase. B. RT-qPCR analysis of top 5 miRNAs in H/R-treated HK-2 cells. C. RT-qPCR analysis of miR-204-5p expression in the sera of PA-AKI patients. D. miR-204-5p interacts with circPICALM by RIP assay. E. starBase predicted binding sites between circPICALM and miR-204-5p. F. Luciferase reporter assay validated the association between circPICALM and miR-204-5p. G. RT-qPCR showed miR-204-5p expression in HK-2 cells after lentivirus transfection. \* $P < 0.05$ ; \*\* $P < 0.01$ ; \*\*\* $P < 0.001$ .

not least, circPICALM from urine or peripheral blood can also be a good biomarker for AKI. We will explore the potential predictive and diagnostic value by constructing a risk predictive model combined with clinical data in the future.

## 6. Conclusion

In summary, the present findings highlight the involvement of circPICALM in PA-induced AKI. Overexpression of circPICALM exacerbated apoptosis, inflammation, and oxidative stress via the miR-204-5p/IL-1 $\beta$  axis in H/R-treated AKI, indicating its contribution to neonatal AKI progression. The insights gained from the present study suggest that early inhibition of circPICALM and then suppression of pro-inflammatory factors could serve as a potential therapeutic target for early intervention in neonatal AKI. Further research is still needed on how circPICALM specifically acts on neonatal AKI, particularly mitochondrial oxidative stress.

## CRediT authorship contribution statement

JJP and YY collected and analyzed the clinical data of the microarray profile regarding AKI. YY was also responsible for subsequent animal model establishment, experiments, and data analysis, and completed a large amount of work including manuscript revision. JJP and XQC were also the contributors in writing and revising the manuscript. JS, MZW, and TYL helped to perform the experiments of qPCR and bioinformatics analysis. JJP made the main contribution to the design of the manuscript

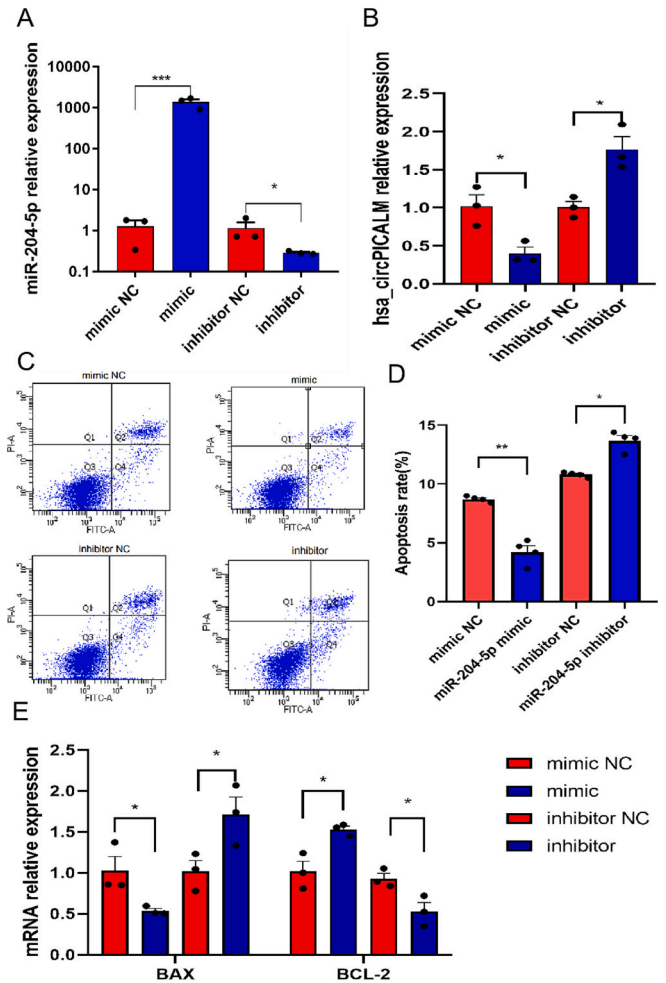


**Fig. 6.** The miR-204-5p mimics attenuated H/R-induced HK-2 cell apoptosis. A–B. RT-qPCR verified miR-204-5p and circPICALM expression after transfection. C–D. Flow cytometry evaluated cell apoptosis in HK-2 cells treated with mimic NC, miR-204-5p mimic, inhibitor NC, and miR-204-5p inhibitor under H/R treatment. E. RT-qPCR analysis of pro-apoptotic BAX and anti-apoptotic BCL-2 expression. \* $P < 0.05$ ; \*\* $P < 0.01$ ; \*\*\* $P < 0.001$ .

and subsequent revisions. XGZ assisted in improving the research design and revising this manuscript. All authors read and approved the final manuscript.

## Consent for publication

All authors listed have read the complete manuscript and approved the paper's submission.

## Ethics approval and consent to participate

This study was approved by the Committee on Human Rights Related to Research Involving Human Subjects, Faculty of Affiliated Children Hospital, Nanjing Medical University (Approved Number: 202107071-1). Informed consent has been obtained from the parents of included newborns. All data were fully anonymized before further statistical analysis. All the procedures were followed by the Declaration of Helsinki.

## Funding

This work was supported by a grant from the Young Talents Startup Fund of Jiangsu Women and Children Health Hospital, China

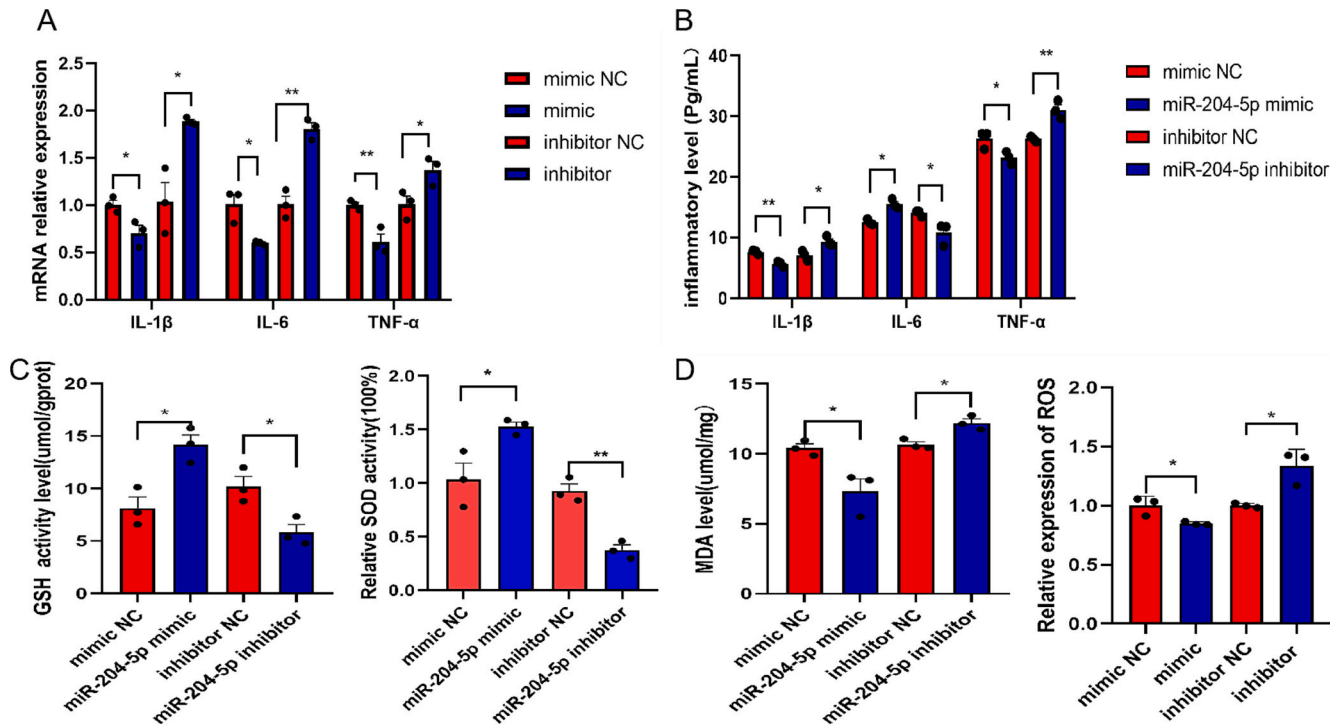


**Fig. 7.** The miR-204-5p mimics attenuated H/R-induced HK-2 cell inflammation and oxidative stress. A. RT-qPCR showed the mRNA levels of IL-1 $\beta$ , IL-6, and TNF- $\alpha$  in HK-2 cells after miR-204-5p mimic/inhibitor transfection. B. IL-1 $\beta$ , IL-6, and TNF- $\alpha$  in HK-2 cells after miR-204-5p mimic/inhibitor transfection by ELISA. C. Levels of antioxidant enzymes GSH and SOD in HK-2 cells after miR-204-5p mimic/inhibitor transfection. D. Levels of MDA and ROS in HK2 cells were measured using the corresponding kits after miR-204-5p mimic/inhibitor transfection. \* $P < 0.05$ ; \*\* $P < 0.01$ .

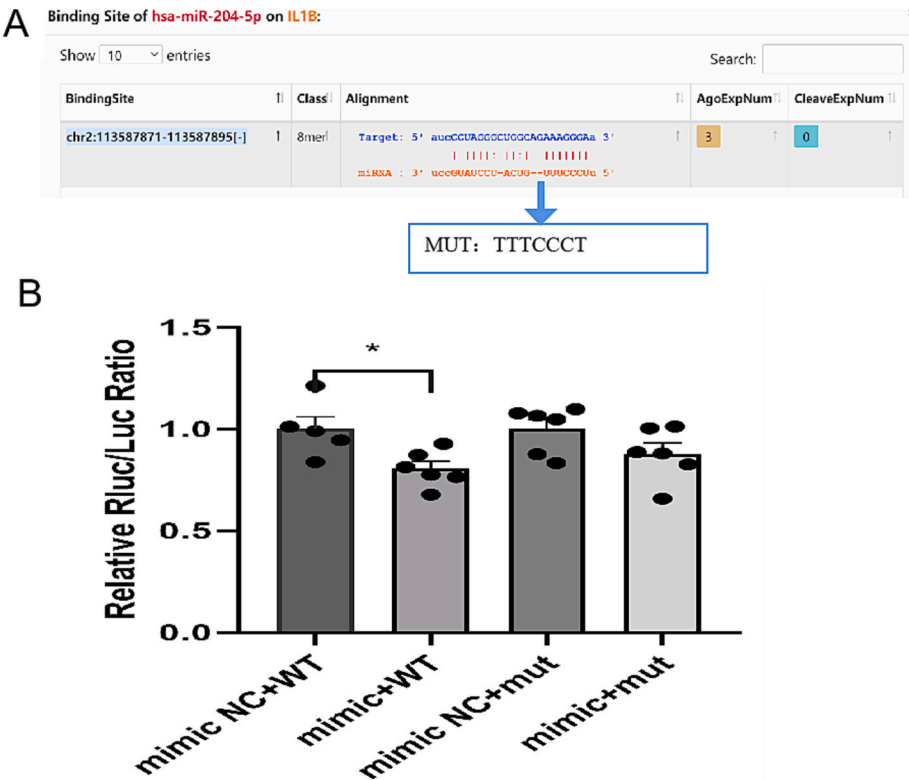


**Fig. 8.** IL-1 $\beta$  was a target of miR-204-5p, and the results of a rescue experiment. A. starBase predicted the binding sites between IL-1 $\beta$  and miR-204-5p. B. Luciferase reporter assay validated the correlation between IL-1 $\beta$  and miR-204-5p. \* $P < 0.05$ .

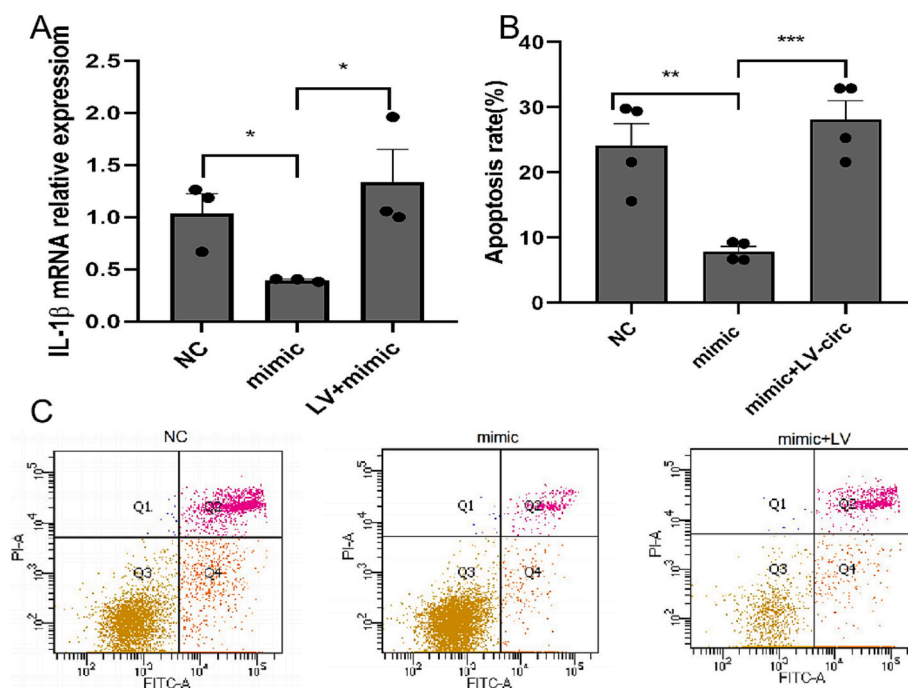


**Fig. 9.** Rescue experiment of circPICALM/miR-204a-5p/IL-1 $\beta$  axis. A. RT-qPCR showed IL-1 $\beta$  mRNA expression in H/R-treated HK2 cells transfected with mimic-NC, miR-204a-5p mimic, or LV-circPICALM+miR-204a-5p mimic. B–C. Flow cytometry evaluated cell apoptosis treated with mimic-NC, miR-204a-5p mimic, or LV-circPICALM + miR-204a-5p mimic. \* $P < 0.05$ ; \*\* $P < 0.01$ ; \*\*\* $P < 0.001$ ; \*\*\*\* $P < 0.0001$ .

(FYRC202012 Q, C.).

## Declaration of competing interest

The authors declare that they have no known competing financial interests or personal relationships that could have appeared to influence the work reported in this paper.

## Acknowledgments

The authors would like to thank the parents of the patients for their understanding, patience, and endurance.

## Appendix A. Supplementary data

Supplementary data to this article can be found online at <https://doi.org/10.1016/j.bbdis.2025.167795>.

## Data availability

The dataset used during this study is available from the corresponding author upon reasonable request.

## References

- J.J. Blinder, L.A. Asaro, D. Wypij, D.T. Selewski, M.S.D. Agus, M. Gaies, M. A. Ferguson, Acute kidney injury after pediatric cardiac surgery: a secondary analysis of the safe pediatric euglycemia after cardiac surgery trial, *Pediatr. Crit. Care Med.* 18 (2017) 638–646, <https://doi.org/10.1097/PCC.0000000000001185>.
- S.K. Gadepalli, D.T. Selewski, R.A. Drongowski, G.B. Mychaliska, Acute kidney injury in congenital diaphragmatic hernia requiring extracorporeal life support: an insidious problem, *J. Pediatr. Surg.* 46 (2011) 630–635, <https://doi.org/10.1016/j.jpedsurg.2010.11.031>.
- S. Kaur, S. Jain, A. Saha, D. Chawla, V.R. Parmar, S. Basu, J. Kaur, Evaluation of glomerular and tubular renal function in neonates with birth asphyxia, *Ann. Trop. Paediatr.* 31 (2011) 129–134, <https://doi.org/10.1179/146532811X12925735813922>.
- R. Koralkar, N. Ambalavanan, E.B. Levitan, G. McGwin, S. Goldstein, D. Askenazi, Acute kidney injury reduces survival in very low birth weight infants, *Pediatr. Res.* 69 (2011) 354–358, <https://doi.org/10.1203/PDR.0b013e31820b95ca>.
- S. Sarkar, D.J. Askenazi, B.K. Jordan, I. Bhagat, J.R. Bapuraj, R.E. Dechert, D. T. Selewski, Relationship between acute kidney injury and brain MRI findings in asphyxiated newborns after therapeutic hypothermia, *Pediatr. Res.* 75 (2014) 431–435, <https://doi.org/10.1038/pr.2013.230>.
- D.T. Selewski, B.K. Jordan, D.J. Askenazi, R.E. Dechert, S. Sarkar, Acute kidney injury in asphyxiated newborns treated with therapeutic hypothermia, *J. Pediatr.* 162 (2013) 725–729.e1, <https://doi.org/10.1016/j.jpeds.2012.10.002>.
- J.B. Carmody, J.R. Swanson, E.T. Rhone, J.R. Charlton, Recognition and reporting of AKI in very low birth weight infants, *Clin. J. Am. Soc. Nephrol.* 9 (2014) 2036–2043, <https://doi.org/10.2215/CJN.05190514>.
- T.Y.D. Mok, M.H. Tseng, J.C. Lee, Y.C. Chou, R. Lien, M.Y. Lai, C.C. Lee, J.J. Lin, I. J. Chou, K.L. Lin, M.C. Chiang, A retrospective study on the incidence of acute kidney injury and its early prediction using troponin-I in cooled asphyxiated neonates, *Sci. Rep.* 10 (2020) 15682, <https://doi.org/10.1038/s41598-020-72717-w>.
- A. Khwaja, KDIGO clinical practice guidelines for acute kidney injury, *Nephron Clin. Pract.* 120 (2012) c179–c184, <https://doi.org/10.1159/000339789>.
- D.T. Selewski, J.R. Charlton, J.G. Jetton, R. Guillet, M.J. Mhanna, D.J. Askenazi, A. L. Kent, Neonatal acute kidney injury, *Pediatrics* 136 (2015) e463–e473, <https://doi.org/10.1542/peds.2014-3819>.
- J.U. Guo, V. Agarwal, H. Guo, D.P. Bartel, Expanded identification and characterization of mammalian circular RNAs, *Genome Biol.* 15 (2014) 409, <https://doi.org/10.1080/15476286.2016.1245268>.
- W.R. Jeck, J.A. Sorrentino, K. Wang, M.K. Slevin, C.E. Burd, J. Liu, W.F. Marzluff, N.E. Sharpless, Circular RNAs are abundant, conserved, and associated with ALU repeats, *RNA* 19 (2013) 141–157, <https://doi.org/10.1261/rna.035667.112>.
- Y. Cao, X. Mi, D. Zhang, Z. Wang, Y. Zuo, W. Tang, Transcriptome sequencing of circular RNA reveals a novel circular RNA-has circ.0114427 in the regulation of inflammation in acute kidney injury, *Clin. Sci. (Lond.)* 134 (2020) 139–154, <https://doi.org/10.1042/CS20190990>.
- M. Kölling, H. Seeger, G. Haddad, A. Kistler, A. Nowak, R. Faulhaber-Walter, J. Kielstein, H. Haller, D. Fliser, T. Mueller, R.P. Wüthrich, J.M. Lorenzen, The circular RNA ciRs-126 predicts survival in critically ill patients with acute kidney injury, *Kidney Int. Rep.* 3 (2018) 1144–1152, <https://doi.org/10.1016/j.ekir.2018.05.012>.
- Y. Xu, X. Li, H. Li, L. Zhong, Y. Lin, J. Xie, D. Zheng, Circ.0023404 sponges miR-136 to induce HK-2 cells injury triggered by hypoxia/reoxygenation via upregulating IL-6R, *J. Cell. Mol. Med.* 25 (2021) 4912–4921, <https://doi.org/10.1111/jcmm.15986>.
- J.J. Pan, Y. Yang, X.Q. Chen, J. Shi, M.Z. Wang, M.L. Tong, X.G. Zhou, RNA sequencing and bioinformatics analysis of circular RNAs in asphyxial newborns with acute kidney injury, *Kaohsiung J. Med. Sci.* 39 (2023) 337–344, <https://doi.org/10.1002/kjm2.12644>.
- D. Yan, W. Dong, Q. He, M. Yang, L. Huang, J. Kong, H. Qin, T. Lin, J. Huang, Circular RNA circPICALM sponges miR-1265 to inhibit bladder cancer metastasis and influence FAK phosphorylation, *EBioMedicine* 48 (2019) 316–331, <https://doi.org/10.1016/j.ebiom.2019.08.074>.

- [18] E. Bona, H. Hagberg, E.M. Løberg, R. Bågenholm, M. Thoresen, Protective effects of moderate hypothermia after neonatal hypoxia-ischemia: short-and long-term outcome, *Pediatr. Res.* 43 (1998) 738–745, <https://doi.org/10.1203/00006450-199806000-00005>.
- [19] D. Alaro, A. Bashir, R. Musoke, L. Wanaiana, Prevalence and outcomes of acute kidney injury in term neonates with perinatal asphyxia, *Afr. Health Sci.* 14 (2014) 682–688, <https://doi.org/10.4314/ahs.v14i3.26>.
- [20] J.R. Charlton, L. Boohaker, D. Askenazi, P.D. Brophy, C. D'Angio, M. Fuloria, J. Gien, R. Griffin, S. Hingorani, S. Ingraham, A. Mian, R.K. Ohls, S. Rastogi, C. J. Rhee, M. Revenis, S. Sarkar, A. Smith, M. Starr, A.L. Kent, Neonatal kidney collaborative. Incidence and risk factors of early onset neonatal AKI, *Clin. J. Am. Soc. Nephrol.* 14 (2019) 184–195, <https://doi.org/10.2215/CJN.03670318>.
- [21] D. Gallo, K.A. de Bijl-Marcus, T. Alderliesten, M. Liliën, F. Groenendaal, Early acute kidney injury in preterm and term neonates: incidence, outcome, and associated clinical features, *Neonatology* 118 (2021) 174–179, <https://doi.org/10.1159/000513666>.
- [22] D.J. Askenazi, P.J. Heagerty, R.H. Schmicker, R. Griffin, P. Brophy, S.E. Juul, D. E. Mayock, S.L. Goldstein, S. Hingorani, PENUT Trial Consortium, Prevalence of acute kidney injury (AKI) in extremely low gestational age neonates (ELGAN), *Pediatr. Nephrol.* 35 (2020) 1737–1748, <https://doi.org/10.1007/s00467-020-04563-x>.
- [23] R. Matsuura, K. Doi, H. Rabb, Acute kidney injury and distant organ dysfunction-network system analysis, *Kidney Int.* 103 (2023) 1041–1055, <https://doi.org/10.1016/j.kint.2023.03.025>.
- [24] S.R. Ma, Q. Ma, Y.N. Ma, W.J. Zhou, Comprehensive analysis of ceRNA network composed of circRNA, miRNA, and mRNA in septic acute kidney injury patients based on RNA-seq, *Front. Genet.* 14 (2023) 1209042, <https://doi.org/10.3389/fgene.2023.1209042>.
- [25] Y. Shi, C.F. Sun, W.H. Ge, Y.P. Du, N.B. Hu, Circular RNA VMA21 ameliorates sepsis-associated acute kidney injury by regulating miR-9-3p/SMG1/inflammation axis and oxidative stress, *J. Cell. Mol. Med.* 24 (2020) 11397–11408, <https://doi.org/10.1111/jcmm.15741>.
- [26] Y. Yang, Z.L. Li, F.M. Wang, R.N. Tang, Y. Tu, H. Liu, MicroRNA26a inhibits cisplatin-induced renal tubular epithelial cells apoptosis through suppressing the expression of transient receptor potential channel 6 mediated dynamin-related protein 1, *Cell Biochem. Funct.* 38 (2020) 384–391, <https://doi.org/10.1002/cbf.3474>.
- [27] R. Kurahashi, T. Kadomatsu, M. Baba, C. Hara, H. Itoh, K. Miyata, M. Endo, J. M. K. Terada, K. Araki, M. Eto, L.S. Schmidt, T. Kamba, W.M. Linehan, Y. Oike, MicroRNA-204-5p: a novel candidate urinary biomarker of Xp11.2 translocation renal cell carcinoma, *Cancer Sci.* 110 (2019) 1897–1908, <https://doi.org/10.1111/cas.14026>.
- [28] J.J. Dong, M. Liu, Y.W. Bian, W. Zhang, C. Yuan, D.Y. Wang, Z.H. Zhou, Y. Li, Y. H. Shi, MicroRNA-204-5p ameliorates renal injury via regulating Keap1/Nrf2 pathway in diabetic kidney disease, *Diabetes Metab. Syndr. Obes.* 17 (2024) 75–92, <https://doi.org/10.2147/DMSO.S441082>.
- [29] Y. Cheng, D.D. Wang, F. Wang, J. Liu, B.R. Huang, M.A. Baker, J.Y. Yin, R. Wu, X. C. Liu, K.R. Regner, K. Usa, Y. Liu, C.X. Zhang, L.J. Dong, A.M. Geurts, N.S. Wang, S.S. Miller, Y.C. He, M.Y. Liang, Endogenous miR-204 protects the kidney against chronic injury in hypertension and diabetes, *J. Am. Soc. Nephrol.* 31 (2020) 1539–1554, <https://doi.org/10.1681/ASN.2019101100>.
- [30] H. Li, J.B. Wang, X.R. Liu, Q. Cheng, MicroRNA-204-5p suppresses IL6-mediated inflammatory response and chemokine generation in HK-2 renal tubular epithelial cells by targeting IL6R, *Biochem. Cell Biol.* 97 (2019) 109–117, <https://doi.org/10.1139/bcb-2018-0141>.
- [31] T. Lakat, A. Fekete, K. Demeter, A.R. Toth, Z.K. Varga, A. Patonai, H. Kelemen, A. Budai, M. Szabo, A.J. Szabo, K. Kaila, A. Denes, E. Mikics, A. Hosszu, Perinatal asphyxia leads to acute kidney damage and increased renal susceptibility in adulthood, *Am. J. Physiol. Ren. Physiol.* 327 (2024) F314–F326, <https://doi.org/10.1152/ajprenal.00039.2024>.
- [32] Y.T. Chen, X.H. Lu, R.L. Whitney, Y. Li, M.J. Robson, R.D. Blakely, J.T. Chi, S. D. Crowley, J.R. Privratsky, Novel anti-inflammatory effects of the IL-1 receptor in kidney myeloid cells following ischemic AKI, *Front. Mol. Biosci.* 11 (2024) 1366259, <https://doi.org/10.3389/fmolb.2024.1366259>.
- [33] Q. Lin, S. Li, N. Jiang, H. Jin, X. Shao, X. Zhu, J. Wu, M. Zhang, Z. Zhang, J. Shen, W. Zhou, L. Gu, R. Lu, Z. Ni, Inhibiting NLRP3 inflammasome attenuates apoptosis in contrast-induced acute kidney injury through the upregulation of HIF1A and BNIP3-mediated mitophagy, *Autophagy* 17 (2021) 2975–2990, <https://doi.org/10.1080/15548627.2020.1848971>.
- [34] Y.J. Liao, X.J. Peng, X.Z. Li, D.K. Wu, S.F. Qiu, X.M. Tang, D.S. Zhang, CircRNA 45478 promotes ischemic AKI by targeting the miR-190a-5p/PHLPP1 axis, *FASEB J.* 36 (2022) e22633, <https://doi.org/10.1096/fj.202201070R>.
- [35] P. Li, Y. Liu, T. You, CircNRIP1 knockdown alleviates lipopolysaccharide-induced human kidney 2 cell apoptosis and inflammation through miR-339-5p/OXSR1 pathway, *Shock* 59 (2023) 426–433, <https://doi.org/10.1097/SHK.0000000000002057>.
- [36] W.D. Ye, Q. Miao, G.X. Xu, K. Jin, X. Li, W.D. Wu, L.N. Yu, M. Yan, CircRNA itchy E3 ubiquitin protein ligase improves mitochondrial dysfunction in sepsis-induced acute kidney injury by targeting microRNA-214-3p/ATP-binding cassette A1 axis, *Ren. Fail.* 45 (2023) 2261552, <https://doi.org/10.1080/0886022X.2023.2261552>.
- [37] L. Cervera-Carles, O. Dols-Icardo, L. Molina-Porcel, D. Alcolea, A. Cervantes-Gonzalez, L. Muñoz-Llahuna, J. Clarimon, Assessing circular RNAs in Alzheimer's disease and frontotemporal lobar degeneration, *Neurobiol. Aging* 92 (2020) 7–11, <https://doi.org/10.1016/j.neurobiolaging.2020.03.017>.
- [38] D. Yan, W. Dong, Q.Q. He, M.H. Yang, L.F. Huang, J.Q. Kong, H.D. Qin, T.X. Lin, J. Huang, Circular RNA circPICALM sponges miR-1265 to inhibit bladder cancer metastasis and influence FAK phosphorylation, *EBioMedicine* 48 (2019) 316–331, <https://doi.org/10.1016/j.ebiom.2019.08.074> (Epub 2019 Oct 21. Erratum in: *EBioMedicine*. 2021 Feb; 64: 103226. doi:10.1016/j.ebiom.2021.103226).